CHAPTER III

SYNTHESIS, GROWTH AND CHARACTERIZATION STUDIES OF NITRAMINO SULPHONIC ACID (NASA) UV NLO CRYSTAL

3. 1. Introduction:

Nonlinear optical crystals play an important role in various advanced scientific and technical areas (Cyranoski 2009) such as resonance ionization spectroscopy (Johnson 1980), plasma production (Mulser 1973), photoacoustic spectroscopy (Ponomarev 2004), launching artificial earth satellite (Ciufolini 1986), remote sensing (Goetz 2007), biology (Bechtel 2014), industries (Nasim 2014), high density optical disk system (Kaneko 1992) etc. due to their higher NLO coefficient. Harmonically generated laser's characteristic properties like directionality, intensity, monochromacity and coherence are specified by the optical nature of NLO medium (crystals). The NLO medium is created by good optical active crystalline materials of organic, inorganic and semiorganic molecules. These crystalline materials are designed by growing them by various growth techniques. Optical transparent organic (Anbarasu 2014), inorganic (Balamurugan 2006, Ji 2013) and semiorganic (Dinakaran 2008) crystals were reported as good NLO materials. Inorganic NLO crystals are explored better than organic crystals for good thermal and mechanical stability and desirable growth nature (Pandian 2008). They can produce larger SHG coefficient, wide transparent region and moderate birefringence and they are incorporated into various laser systems for harmonic generation and optoelectronic switching (Hu 2003, Balamurugan 2006). Beside phosphate and borate classes, amino based inorganic crystals having good SHG efficiency also were grown (Lenin 2007, Bindhu 2012, Ramesh Babu 2010).

Amino acid combined with nitro functionality crystallizes in noncentrosymmetric space group and can produce piezoelectric effect and SHG (Valenzuela 2009, Vizhi 2013), such that these two molecular moieties are interesting for NLO applications. Energetically active nitramino substituted compounds are intense fascination of scientists and technologists due to their potential importance to prepare sensitive/insensitive materials in Defense laboratories (Duddu, 2010, Singh 2007). The energetic performance is more in nitramino compounds in regard to intermolecular force interactions, oxygen balance, density and other thermodynamic properties. Such nitramino derivatives of aromatic compounds (Duddu 2010, Klapotke, 2009) were synthesized and characterized. The dissociation energy of N-NO_2 bond was estimated as 49.4 $kcalmol^{-1}$ through B3/PW91 DFT calculations while studying energetic behaviors in nitramino substituted compound (Politzer 1996). Protonation of amino compounds with concentrated HNO_3 yields nitramino molecules (Klapotke 2009). Nitramino-functionalized crystals possess high densities, high positive heats of formation, and good oxygen balance (Fischer 2015). Azoles were energized with aid of nitramino group and crystallized by acidic nitration conditions (Fischer 2015). Furazan was functionalized with nitramino and crystallized (Tang 2015). Pyrazoles were functionalized with N-nitramino energetic moity and crystallized (Yin 2016).

Sulphamic acid crystallized as zwitterionic molecule ($NH_3^+SO_3^-$) of a distorted tetrahedral in the solid state form but it is a strong monobasic acid in aqueous solution with H_2N-SO_2-OH structure (Kanda 1951). In the zwitterionic form, the bond angles of N-S-O and O-S-O are deviated from normal tetrahedral value due to repulsive/attractive forces among negatively charged oxygen atoms and positively charged ammonia ion.

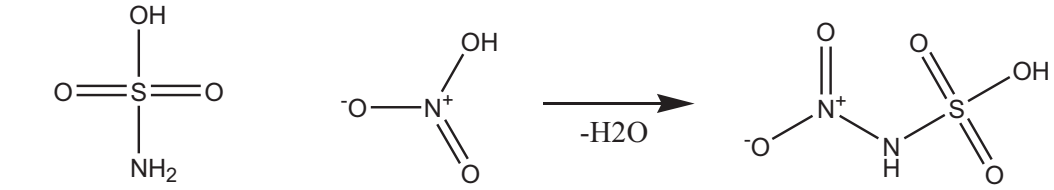

Fig. 3. 1. Reaction scheme of NASA

The strong lattice force due to $–NH_2$ bond accounts to its melting point is 206 º higher than other sulphonic acids. Sulphonic acid substituted materials are highly sensitive in metal ion detecting (Roy 2013). The super acidic-ionic liquids (Dupont 2016) have been recently prepared by mixing the N-alkylated sulphamic acid with Bistriflimic acid (Dupont 2016). The kinetics in reaction of sulphamic acid with nitrous acid (Hughes 1967) and nitric acid (Hughes 1977a) was studied. Recently 2, 3-amino-4-amidoximinofurazan reacted with fuming nitric acid and yielded energetic crystals grown by slow solvent evaporation technique (Sun 2018). These findings encouraged to mix amino sulphonic acid (sulphamic acid) and nitric acid to explore a new hybrid material nitramino sulphonic acid (NASA), to characterize its structural, optical, dielectric and mechanical properties and to make nitramino as explosively insensitive as well as optically energetic by stabilizing it within sulphonic acid host molecules.

3. 2. Experimental Techniques:

3. 2. 1. Chemicals

Sulphamic acid (Amino sulphonic acid) (99% pure AR grade) and Concentrated Nitric acid (99.5% pure AR grade) were purchased from E-merck Co Ltd.

3. 2. 2. Synthesis of NASA

NASA was synthesized using the typical synthetic method approached (Martin 1977). Sulphamic acid and nitric acid was taken in equimolar ratio. Nitric acid was added drop by drop with sulphamic acid. The resultant mixture was heated up to 79^oC temperature and agitated using a magnetic stirrer for an hour and then cooled to ambient temperature. White colored precipitates were obtained at the bottom of the beaker. Fig. 3. 1 shows the reaction scheme for preparing NASA crystalline salt.

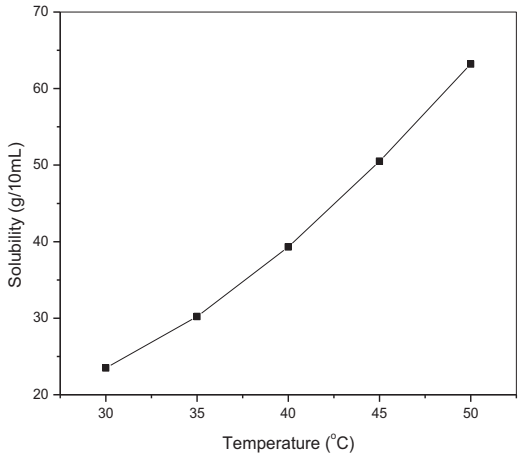

Fig. 3. 2. Solubility curve of NASA

3. 2. 3. Solubility study

The synthesized salt was used to measure the solubility of NASA crystal in water. A 250 ml borosil glass beaker filled with 100 ml water was placed inside a constant temperature bath. An acrylic sheet with a circular hole at the middle was placed over the beaker through which a spindle from an electric motor, placed on the top of the sheet was introduced into the solution. A Teflon paddle was attached at the end of the rod for stirring the solution. The synthesized salt was added in small amounts with water and stirring was continued till the formation of precipitate, which confirmed the supersaturation of the solution. A 20 ml of the saturated solution was withdrawn by means of a warmed pipette and the same was poured into a clean, dry and weighed Petri dish. The solution was kept in a heating mantle for slow evaporation till the whole of the solution got evaporated and the mass of the NASA salt in 20 ml of solution was determined by weighing the Petri dish with salt and hence the solubility, i.e quantity of salt in grams dissolved in 100 ml of the solvent was determined. The solubility of NASA in doubly deionized water was determined for five different temperatures (30, 35, 40, 45 and 50 ^{o}C) by adopting the same procedure. The resulting solubility curve of pure NASA is shown in Fig. 3. 2.

3. 2. 4. Crystal growth technique

The saturated solution of NASA in aqueous medium was prepared by dissolving the purified crystalline salt of NASA in doubly deionized water at 30^{o}C. The saturated solution of 200 ml was taken in a 250 ml borosil beaker and properly sealed and then placed in the constant temperature water bath. The solvent was slowly evaporated. Nucleation was started after a week.

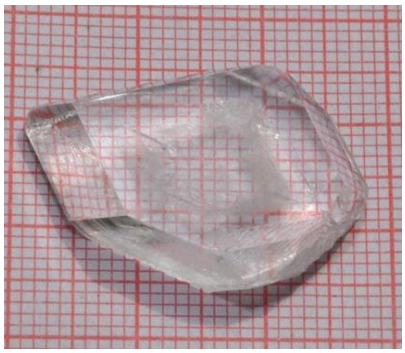

Fig. 3. 3. Photograph of as grown NASA UV NLO Crystal

Good quality single crystals were harvested in a period of 30 days. The NASA crystal of dimension (26 x 20 x 10 mm^3) grown by slow solvent evaporation technique is shown in Fig. 3. 3.

3. 3. Result and Discussion

NASA crystal was subjected to the following studies:

i. Single crystal X-ray Diffraction analysis (XRD) for measuring unit cell parameters.

ii. High Resolution XRD study to trace out the crystalline purity.

iii. X-ray Powder Diffraction analysis (XRPD) to identify the crystalline phase with crystallinity.

iv. FTIR analysis to trace out the spectral map and confirm the various functional groups present in NASA molecule.

v. UV-Vis-NIR analysis to study the optical absorption behavior of NASA crystal and to calculate its optical band gap energy.

vi. Dielectric measurement technique to investigate the dielectric response of NASA for various frequency range

vii. Photoconductivity study to measure the photoresponsiveness of the crystal

viii. NLO test to check the non-linear response of the crystal to the incident coherent light.

ix. The phase matching between illuminated laser beams and second harmonic waves generated from NASA crystalline medium was identified.

x. Vicker's microhardness test to study the harness of the NASA crystal

3. 3. 1. Single crystal X-ray diffraction:

In order to determine the cell parameters and space group, the single crystals of NASA were subjected to single crystal X-ray diffractometer (Model: Bruker-Nonius Kappa Apex II CCD) with Mo radiation of wavelength $\lambda = 0.71073$ Å. Lattice parameters of NASA was found that a = 8.0617 Å, b = 8.1116 Å, c = 9.2310 Å , $\alpha = 90^o$, $\beta = 90^o$, $\gamma = 90^o$ and V = 603.6454 $Å^3$. From the X-ray diffraction data, it is observed that NASA belongs to orthorhombic crystal system with space group P_{ba2} which is noncentro-symmetric, thus satisfying one of the basic and essential material requirements for SHG activity of the crystal.

3. 3. 2. High Resolution XRD study

Fig. 3. 4 shows the high-resolution diffraction curve (DC) recorded for a typical NASA single crystal specimen using (012) diffracting planes in symmetrical Bragg geometry with $MoK\alpha_1$ radiation. As seen in the figure, the DC contains a single peak and indicates that the specimen is free from structural grain boundaries. The full width at half maximum (FWHM) of this curve is 10 arc s which is quite close to that expected from the plane wave theory of dynamical X-ray diffraction(Batterman 1964) and reveals the presence of point defects and their aggregates. It is interesting to see the shape of the DC. The DC is asymmetric with respect to the Bragg peak position.

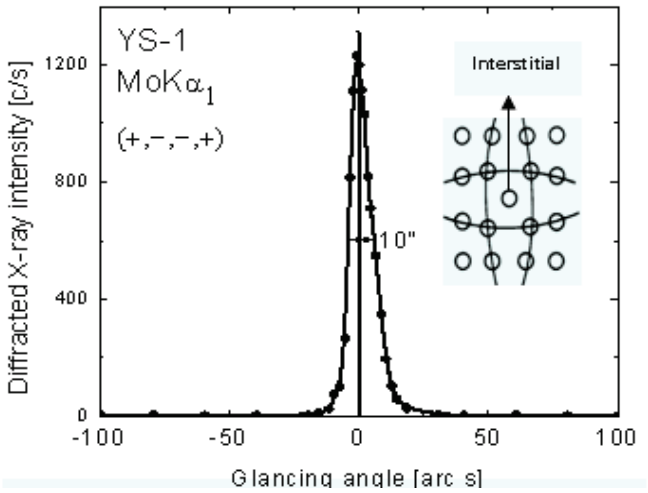

Fig. 3. 4. DC recorded for NASA UV NLO crystal using (012) diffracting planes. Insert shows the schematic of a interstial defect

For a particular angular deviation ($\Delta\theta$) of glancing angle (θ) with respect to the Bragg peak position (taken as zero for the sake of convenience), the scattered intensity is much more in the positive direction in comparison to that of the negative direction. This feature clearly indicates that the crystal contains predominantly interstitial type of defects than that of vacancy defects. This can be well understood by the fact that due to interstitial defects, the lattice around these defects undergo compressive stress (Bhagavannarayana 2008) and the lattice parameter d (interplanar spacing) decreases and leads to give more scattered (also known as diffuse X-ray scattering) intensity at slightly higher Bragg angles (θ_B) as d and sin θ_B are inversely proportional to each other in the Bragg equation ($2d \sin \theta_B = n\lambda$; n and λ being the order of reflection and wavelength respectively which are fixed). The inset in the curve shows the schematic to illustrate how the lattice around the defect core undergoes compressive stress. The converse explanation is true in case of vacancy defects which cause tensile stress in the lattice around the defect core leading to increase of lattice spacing and in turn results in more scattered intensity at the lower Bragg angles. It may be mentioned here that the variation in lattice parameter is confined very close to the defect core which gives only the scattered intensity close to the Bragg peak. Long range order could not be expected and hence change in the lattice parameter is also not expected (Bhagavannarayana 2010). It may be worth to mention here that the defects are more or less statistically distributed in the crystal. If the defects are not statistically distributed but distributed here and there as macroscopic clusters, then the strain generated by such clusters is larger leading to cracks and structural grain boundaries which can be seen very clearly in HRXRD curves with additional peak(s) as observed in our recent study on urea-doped crystals in ZTS at various levels of doping (Bhagavannarayana 2011).

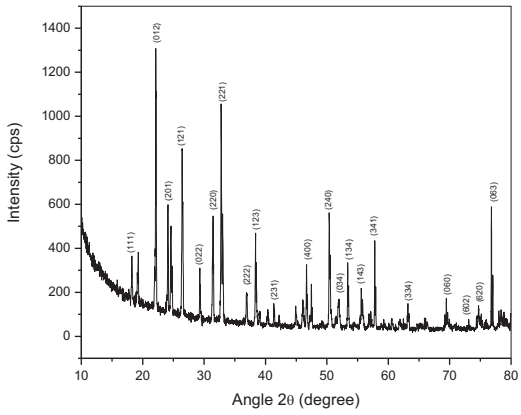

Fig. 3. 5. Powder XRD pattern of NASA UV NLO Crystal

However, in the present experiments the diffraction curve does not contain any additional peak and indicates the absence of clustering of point defects at macroscopic level. The single diffraction peak with reasonably low FWHM indicates that the crystalline perfection is quite good.

3. 3. 3. Powder X-Ray Diffraction Analysis

The powder sample of NASA crystal was subjected to powder X-ray diffraction studies with Riech Single X-ray diffractometer using CuKα radiation of wavelength λ = 1.5418 °A over the range of 10–80° with a scan speed of 0.2°/s. The powder XRD pattern is shown in Fig. 3. 5 and it assures the structural perfection and purity of as grown NASA single crystal. By applying the lattice parameter values obtained from single crystal XRD, (hkl) values were simulated and the (hkl) index of the corresponding reflecting planes were enumerated by manual indexing (Hesse 1948).

3. 3. 4. FTIR Analysis

The FTIR spectrum was recorded in the range 400–4000 cm^{-1} employing Bruker model IFS 66 V FTIR spectrometer by KBr pellet technique. The recorded FTIR spectrum of nitric acid doped SA single crystal is shown in Fig. 3. 6. The stretching vibrations of hydrogen bonds present in sulfonic host molecules are observed in the regions centered 3400 cm^{-1} for SO_2-N-H stretching and centered 900 for SO_2-O-H stretching vibrations (Silvestein 2005). The strong peaks at 3142 cm^{-1} and 1002 cm^{-1} are due to the stretching vibrations due to N-H and O-H hydrogen bonds. The observed peak at 2873 cm^{-1} is attributed to N-H….O vibration. The broad envelop of peaks belonging to the range 1350-1250 cm^{-1} corresponds to the degeneracy of SO_3^- stretching (Ramesh Babu 2010).

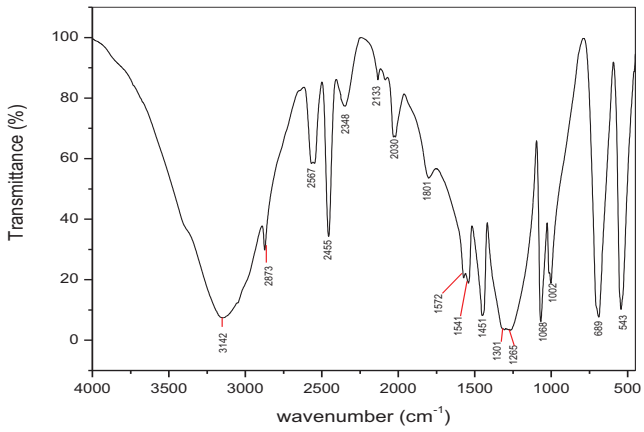

Fig. 3. 6. FTIR spectrum of NASA UV NLO Crystal

The peak positioned at 1265cm^{-1} proved degeneracy of SO_3^- stretching. Symmetric stretching mode of SO_3 is observed at 1068cm^{-1}. The N-S stretching coupled with SO_3 rocking is found at the peak at 689 cm^{-1}. The NH_3^+ rocking mode vibration is observed at 1068 cm^{-1}. Aliphatic nitro compounds transmit the energy in the region 1600 to 1530 cm^{-1} by asymmetric stretching and in 1390 to 1300 by symmetric stretching. The peaks at 1572, 1541 and 1315 cm^{-1} confirm the nitro stretching. In general, symmetric and asymmetric stretching mode vibrations of S=O in sulfonamide and sulfonic acid (anhydrous) compounds are observed in the regions 1350-1325 cm^{-1} and 1150-1140 cm^{-1} respectively. The peaks observed at 1315 and 1265 cm^{-1} assure the S=O stretching. The peaks at 1572 cm^{-1} and 1541 cm^{-1} are corresponding to N-H bending mode vibration (Pavia 2009).

3. 3. 5. UV-vis-NIR analysis

UV-vis-NIR spectral study is a useful tool to measure the optical transparency which is a most important for laser generative material. Optical transmittance spectrum was recorded using Varian Cary 5E-UV-vis-NIR spectrometer in the wavelength region of 200 – 800 nm. Fig. 3. 7 shows the plot of transmittance against the wavelength. The transmittance in the entire visible region is about 90%. The lower cut-off wavelength of NASA crystal is at 290 nm. The optical absorption coefficient (α) was calculated from the transmittance using the relation

$$\alpha = (2.3036/d) \log(1/T) \qquad \text{-------- (1)}$$

where d is the thickness of the crystal and T is the transmittance.

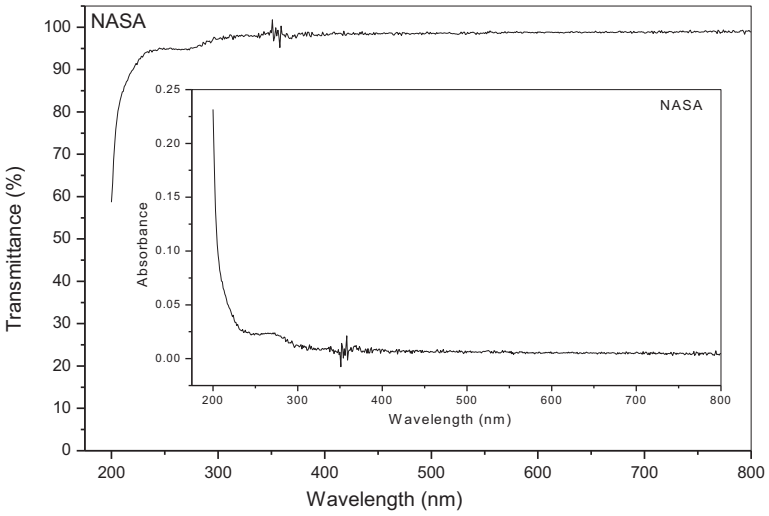

Fig. 3. 7. Optical transmittance of NASA UV NLO Crystal. The insert is the absorbance spectrum

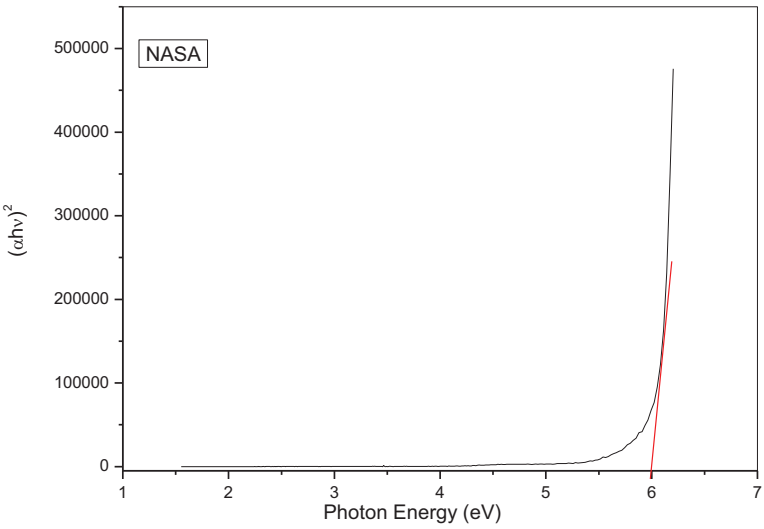

Fig. 3. 8. Tauc's Plot for direct optical band gap energy of NASA UV NLO Crystal

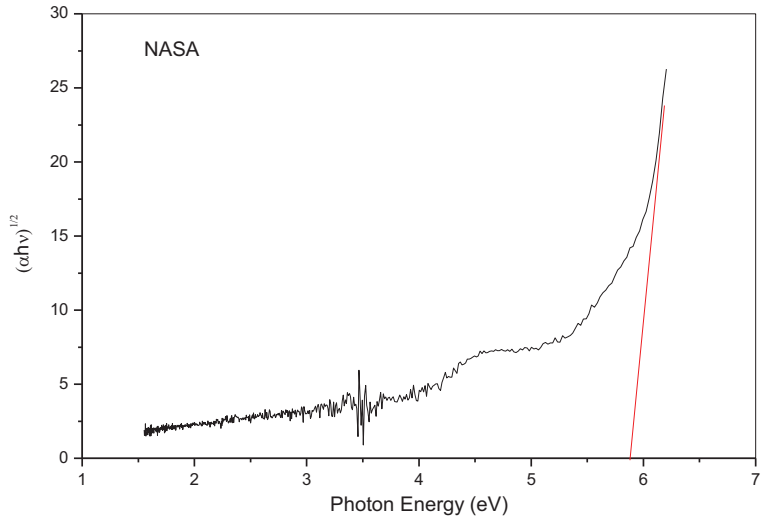

Fig. 3. 9. Tauc's Plot for indirect optical band gap energy of NASA UV NLO Crystal

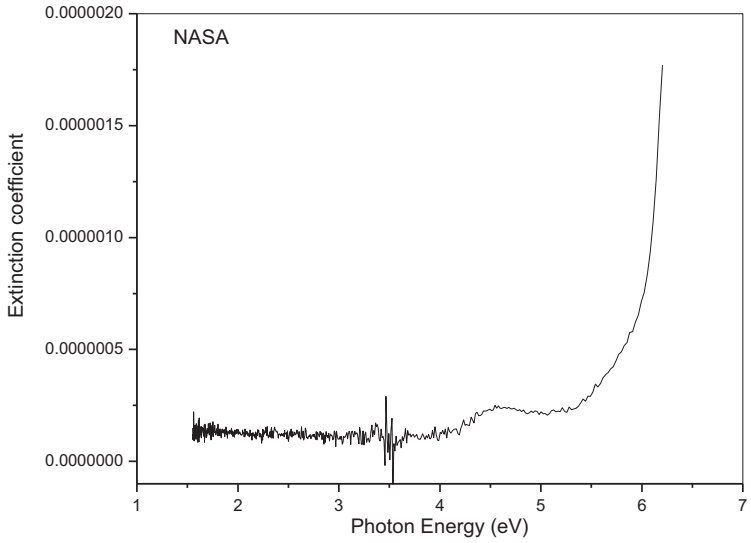

Fig. 3. 10. Plot of Extinction coefficient of NASA UV NLO Crystal

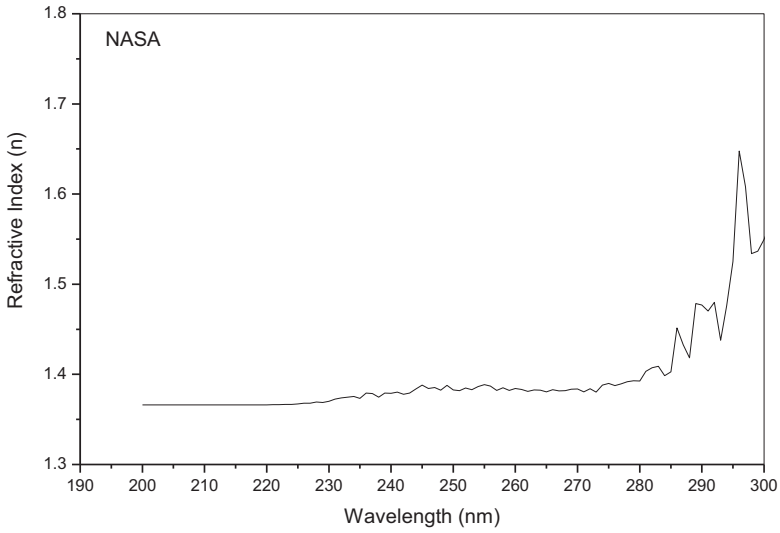

Fig. 3. 11. Plot of Refractive Index of NASA UV NLO Crystal

The optical band gap E_g is calculated from the Tauc's expression,

$$(\alpha h\nu)^n = A(h\nu - E_g) \quad \text{---------} \quad (2)$$

where α is the absorption coefficient, A is disorder parameter. E_g is calculated from the plot $(\alpha h\nu)^n$ versus hν. For the direct band gap energy n = 2 and for the indirect band gap energy n= (1/2). Fig. 3. 8 & Fig. 3. 9 show the plot for direct transition and indirect transition respectively. From the graph it was observed that the direct band gap energy $E_{g(direct)}$ = 6.10 eV and indirect band gap energy $E_{g(indirect)}$ = 5.87 eV. This enhances the NASA crystal for laser generation and other NLO applications. As can be seen from the band gap energy values, direct band gap energy is higher than indirect. The extinction coefficient of NASA crystal was plotted against the energy as shown in Fig. 3. 10 and the refractive index was plotted against wavelength as shown in Fig. 3. 11. NASA exhibits low extinction coefficient and low refractive indices in UV region.

3. 3. 6. Dielectric measurement

The dielectric behavior correlated with electro-optic properties in the crystal reveals the information about the electric field distribution and charge transport mechanism (Viswanathan 2009). The dielectric studies of the NASA crystal was carried out using HIOKI 3532 LCR HITESTER instrument in the frequency region of 50 Hz to 5 MHz at various temperatures of 40, 50, 60 and 70^oC. The cut and smoothly polished crystal piece of thickness 1mm was covered by silver paste and then mounted between two electrodes. The capacitance of the parallel plate capacitor with the sample as the dielectric medium was measured at the temperature region varying from 40-70^oC in steps of 10^oC.

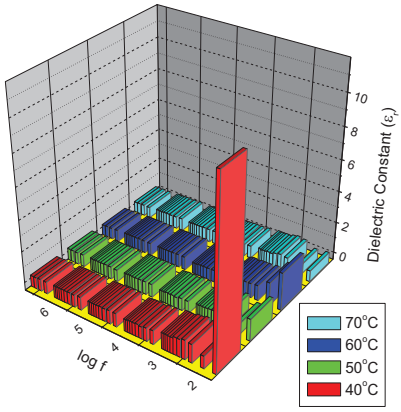

Fig. 3. 12. Plot of Dielectric constant of NASA UV NLO Crystal

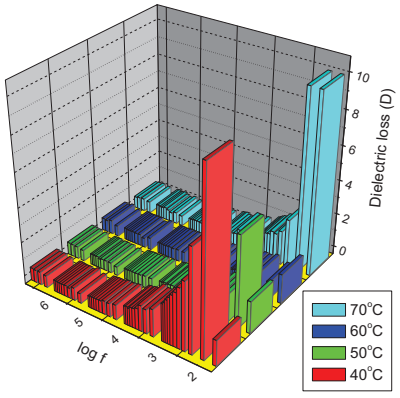

Fig. 3. 13. Plot of Dielectric loss of NASA UV NLO Crystal

The dielectric constant (ε_r) was calculated using the relation

$\varepsilon_r = Cd/\varepsilon_o A$ -------- (3)

where C is the capacitance, d is the thickness of the crystal, ε_o is the permittivity of the free space and A is the area of the crystal surface. The dielectric loss was also calculated. Fig. 3. 12 & Fig. 3. 13 show the variation of the dielectric constant and dielectric loss respectively with respect to the frequency at various temperatures. From the graph it is found that dielectric constant and dielectric loss decrease with increasing frequency. The four important ionic, electronic, dipolar and space charge polarizations contribute the peculiar dielectric behaviors to the crystal. Due to the charged lattice defects, space charge polarization attributes the larger values of dielectric constant at lower frequency. The dielectric constant attains saturation at higher frequencies. At 40 ^oC temperature, the dielectric constant is high at low frequency. Te value of dielectric constant decreases when temperature increases. This is due to the temperature dependent dipolar polarization which change molecule's orientation in crystal lattice since the dipoles may be 'frozen in' at low temperatures (Kurtz 1968). This behavior enhances NASA as the potential candidate for photonic, laser and other NLO devices.

3. 3. 7. Photoconductivity study

Keithley 485 pico ammeter measured the photoconductivity NASA samples. Initially, the sample was kept away from any other radiations. The crystal sample was connected in series to a DC power supply and pico ammeter. Silver paint was coated on sample to make the electrical contacts. The radiation from a halogen lamp containing iodine vapour was exposed on the sample by focusing a spot of light on the sample with the help of a convex lens.

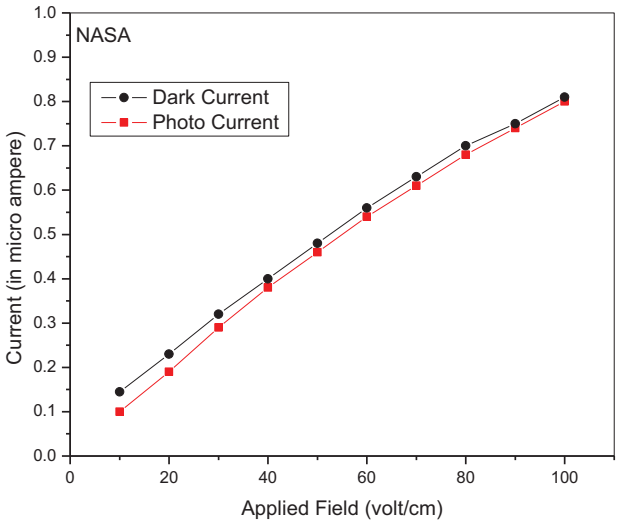

Fig. 3. 14. Photoconductivity of NASA UV NLO Crystal

The photocurrent (I_p) was calculated. Initially the applied voltage was increased from 0 to 100 V in steps of 20 V and the corresponding dark currents were measured. Fig. 3. 14 shows the plot of variation of both the dark current and photo current of the sample against the applied voltage. Both the dark and photocurrent were seen to increase linearly with the applied field. For the same applied field, the photo current is less than the dark current which reveals the negative photo conducting behaviour of NASA single crystal.

3. 3. 8. SHG measurement

The primary widely used technique for confirming the second harmonic generation (SHG) from prospective second order NLO material is the Kurtz-Perry powder technique (Kurtz 1968) High intensity Q-switched Nd:YAG laser (λ = 1064 nm) with input laser energy of 0.68 J was used to illuminate the NASA crystalline powder. The SHG was confirmed by the NASA emitting the green radiation (532 nm). The output SHG efficiency of NASA is nerely 1.6 times of standardd KDP crystal. Thus NASA is confirmed as a suitable NLO medium for laser generation.

3. 3. 9. Phase Matching study

NASA crystalline sample was ground and sieved into distinct particle sizes in the range of less than 106, 106-125, 125-150 and above 150 μm. KDP crystal was also sieved into the particle dimension of NASA. Q-switched Nd:YAG infrared laser pulses irradiated on the sieves. SHG efficiency depends on the particle size and varies with size of sieves. SHG output was measured and plotted for various particle size. SHG intensities increased with increasing particle size upto 150 μm as shown in Fig. 4. 15. It confirms the phase matching behavior of NASA. It is a promising phase matchable NLO crystal for LASER generation.

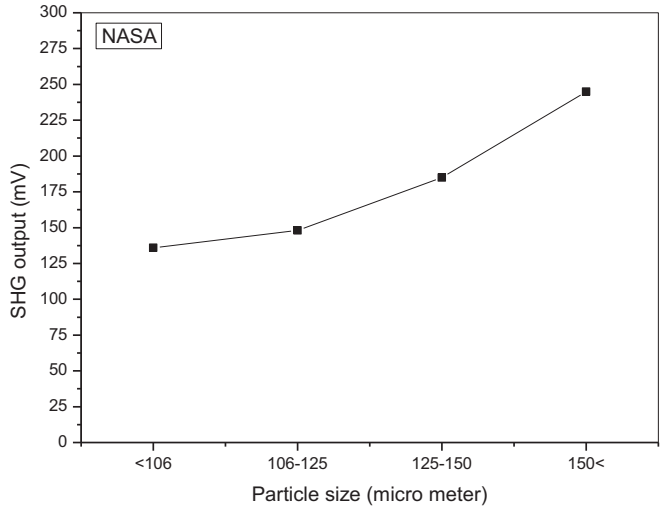

Fig. 3. 15. Phasematching curve of NASA UV NLO Crystal

3. 3. 10. Microhardness Test

Leitz Wietzlar Vickers Microhardness tester measured the hardness parameters of single crystal of NASA at room temperature. Flat shape crystal was fitted with a Vickers diamond pyramidal indenter light microscope. The static indentations were made at room temperature with a constant indentation time of 15 seconds for all indentation. The indenter marked on the crystal surfaces by varying the load from 20 to 100 g. The Vickers microhardness number H_v of the crystal was calculated using the relation

$$H_v = 1.8544\ P/d^2\ Kg\ mm^{-2} \quad \text{---------- (4)}$$

where P is the applied load and d is the average diagonal length of the indented impression in mm. Vickers microhardness profile as a function of load is shown in Fig. 4. 16. (a)

By using Meyer's law, the load P is related with the indentation size as

$$P = k_1 d^n \quad \text{---------- (5)}$$

Mayer constant (k_1) and work hardening coefficient (n) are the constants for a particular sample. The work hardening coefficient n is calculated from the slope of the curve drawn by plotting log (P) against log (d) as shown in Fig. 4. 16 (b)

The value of k_1 was measured from the derivative of the curve drawn by plotting P against d^n as shown in Fig. 4.16 (c). The value of n is found to be 2.45.

If n is greater than 2, the microhardness number H_v increases with increasing load (Onitsch 1947, Hanneman 1941), The work hardening coefficient value of NASA proves that NASA is a soft material.

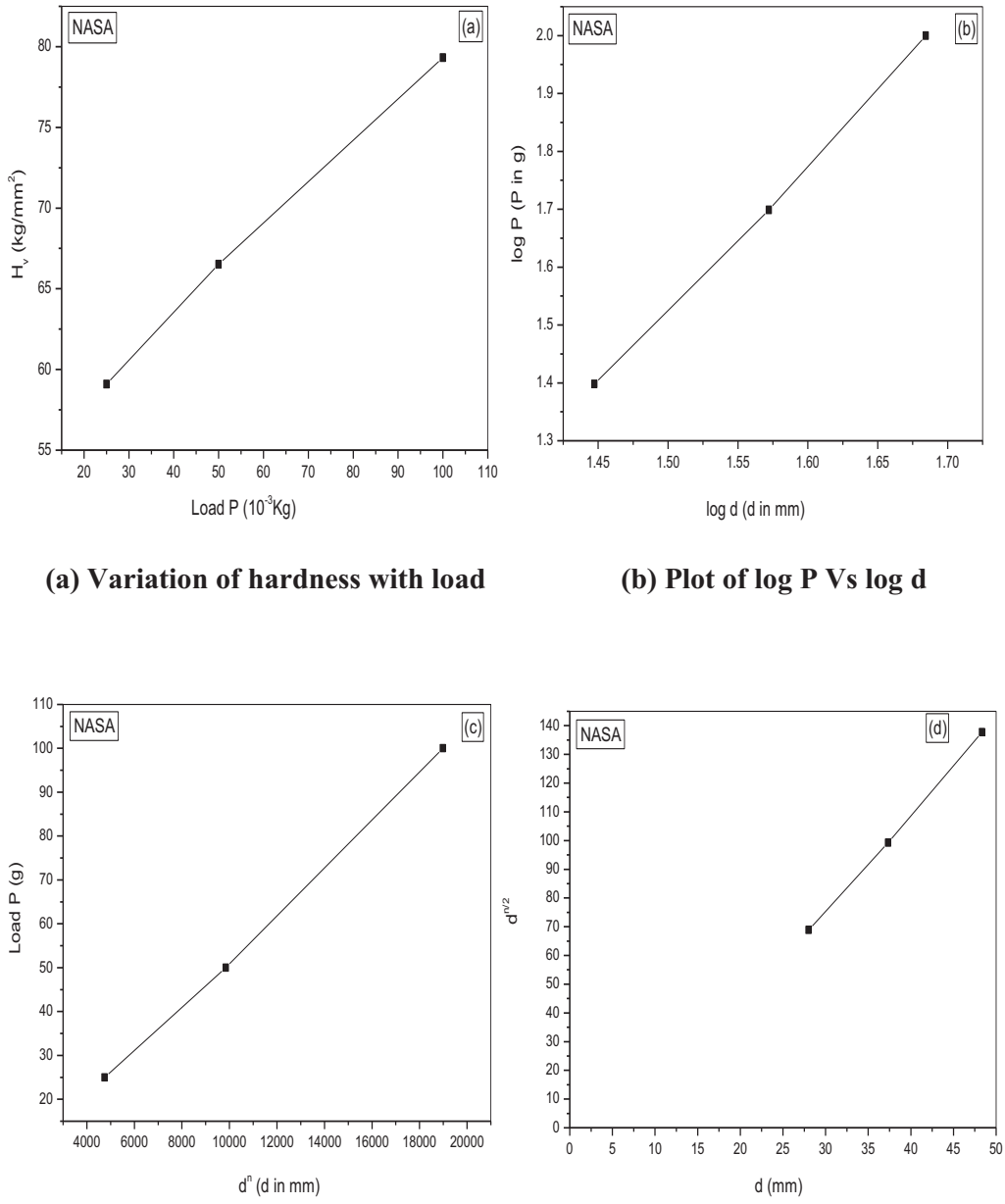

(a) Variation of hardness with load **(b) Plot of log P Vs log d**

(c) Plot of d^n Vs P **(d) Plot of log d Vs $d^{n/2}$**

Fig. 3. 16. Microhardness measurements of NASA single crystal. (a) Variation of harness with load, (b) Plot of log P versus log d, (c) Plot of d^n versus P, (d) Plot of d versus $d^{n/2}$.

Table 3. 1. Hardness Parameters of NASA UV NLO Crystal

Hardness Parameters	Calculated Value
N	2.54
k_1	5.19 (10^{-3} Kg)
k_2	58.94 (10^{-3} Kg)
X	12 (μm)
σ_v	16.32 (MPa)

The degree of dislocation density of the material is related with load P and indentation d through Kick's law given by

$P = k_2(d+x)^2$ ---------- (6)

simplifying Eqn. (5) and (6) we get

$d^{n/2} = (k_2/k_1)^{1/2} d + (k_2/k_1) x$ ---------- (7)

$d^{n/2}$ is plotted against d as shown in Fig. 4.16(d) and the slope of the straight line yields $(k_2/k_1)^{1/2}$ and the intercept is a degree of x.

The yield strength of the material is given by

$\sigma_v = (H_v/2.9)\{[1-(2-n)] \times [(12.5)(2-n)/(1-(2-n))]^{2-n}\}$ ---------- (7)

From the graphs, the constants k_1, k_2 and x are evaluated and the yield strength (σ_v) of NASA is computed. Hardness parameters of NASA crystal are tabulated in Table 3.1. As the work hardening coefficient value of NASA is n=2.45, it suggests that NASA is a soft material.

3. 4. Conclusion:

New laser NLO (nonlinear optical) inorganic material nitramino sulphonic acid (NASA) [$H_2N_2SO_5$] was synthesized and grown from aqueous solution by slow solvent evaporation technique at room temperature. Single crystal XRD revealed that NASA crystallizes in orthorhombic noncentrosymmetric space group P_{ba2}. The structural purity was confirmed by powder XRD. The crystalline perfection of the grown crystal was analyzed by High resolution XRD. Molecular functional groups in NASA were identified by FTIR spectral analysis. UV-vis-NIR spectral study revealed the NASA has good value 6.10 eV of direct band gap energy. Dielectric measurement elucidates NASA has lesser defects. Owing to its higher SHG efficiency, NASA is considered as a promising material for Laser generation. Nitramino molecular moiety is optically energetic for laser generation. It is a phase matchable second order NLO crystal with SHG efficiency to 1.6 times that of KDP. Soft crystal growth habit made it feasible to process. NASA is a UV transmittable crystal suitable for various energy harvesting processes. Explosive sensitive destable nitramino bond was converted to optically energetic by stabilizing N-NO_2 bond within sulphonic acid host molecules.